Electrochemical Nanostructuring with Ultrashort Voltage Pulses

VIOLA KIRCHNER, XINGHUA XIA,† AND ROLF SCHUSTER*

Fritz-Haber-Institut der Max-Planck-Gesellschaft, Faradayweg 4-6, D-14195 Berlin, Germany

Received July 18, 2000

ABSTRACT

The application of nanosecond voltage pulses to electrodes provides three ways to conduct local electrochemistry on the micro- to nanometer scale. (1) The finite charging time of the double-layer capacity allows the machining of three-dimensional microstructures. (2) In an electrochemical scanning tunneling microscope, reactions are confined to the tunneling region, due to the depletion of the electrolyte in the tip−surface gap. (3) Ordering processes, following very fast electrochemical reactions, lead to unconventional island patterns on a surface.

I. Introduction

The physical properties of nanostructured materials differ in general very much from those of the macroscopic bulk material. Electrons confined in small semiconductor crystallites exhibit discrete energy levels rather than bands, which rendered materials consisting of such small "quantum dots" to be of particular interest for the fabrication of, e.g., electro-optic devices.[1−3] Also, the catalytic activity of metals strongly depends on their size, which reflects the correlation between electronic structure and chemical bonding of the adsorbates.[4] However, it is not only the particle size and shape which determine the characteristics. The arrangement of the nanoparticles also influences their properties. In quantum dot lasers, the lateral coupling between the electronic states depends crucially on a well-defined distance between the quantum dots.[5,6] Therefore, one of the most important technological goals is to tailor materials according to the desired properties. This can be performed in two principally different ways. First, the structures can be assembled or manufactured part by part. The other possibility is to exploit the "self-organization" of a system, e.g., upon ordering processes following a phase transition or the pattern formation in dissipative systems.[7]

Recently, also electrochemical methods became important in this respect because of both the well-established chemical procedures for fabrication of nanoparticles and the ease of supplying materials dissolved in an electrolyte. For example, photoactive quantum dots of CdS were synthesized on a graphite surface.[8,9] In modern device technology, electrochemical Cu deposition is currently applied for establishing the on-chip interconnections to overcome the technological problem of coating structures with high aspect ratios.[10]

All this triggered recent efforts to combine electrochemical methods with nanostructuring techniques, by which well-defined patterns are formed on a surface. Among these new techniques is the scanning electrochemical microscope,[11−13] in which a microelectrode is positioned in front of a surface. Electrochemical reaction products formed at this electrode then diffuse toward the surface and, e.g., etch the surface locally. However, the size of the structures is determined by the diffusion length of the reactive species, and hence the local resolution is rather in the range of micrometers, even with very tiny electrodes. Direct electrochemical modification of the surface by local oxidation or reduction has also been achieved, mostly with fairly limited spatial resolution. This points to a general problem which hampers the improvement of the resolution in electrochemical nanostructuring: Electrochemical reactions are governed by the potential drop within the very thin electrochemical double layer (DL) at the electrode surface.[14] Upon application of an external voltage, the ions in the solution redistribute and the potential varies essentially across the DLs, which—in concentrated electrolytes—can be considered as plate capacitors with very thin dielectrica of about one water molecule thickness. The electrolyte provides an effective shortcut between the DLs on the two electrodes. Therefore, the local thickness of the electrolyte, i.e., the shape of the electrodes, has only a weak influence on the reaction rate.

To overcome this constraint, we performed experiments in which we applied very short voltage pulses of only 10 to about 1000 ns duration to a tool electrode in the proximity to the workpiece to be structured. The structuring was achieved in three principally different ways. The first employed the finite time for polarizing the DL, given by the DL capacity and the finite electrolyte resistance. The electrolyte resistance is proportional to the

Viola Kirchner obtained her diploma in chemistry from the Free University of Berlin, Germany, in 1997. She is currently working on electrochemical microstructuring of metals and semiconductors as a Ph.D. student at the Fritz-Haber-Institute of the Max-Planck-Society (FHI), Berlin.

Xinghua Xia obtained his M.Sc. in chemistry from Xiamen University, P.R. China, in 1989. After graduating with a Ph.D. on electrocatalysis on Pt surfaces in 1996 in the group of Prof. W. Vielstich at the University of Bonn, Germany, he joined R. Schuster's group at the FHI, Berlin, for a postdoctoral stay in 1997. He is currently working on semiconductor electrochemistry with Prof. J. J. Kelly, University of Utrecht, Netherlands.

Rolf Schuster obtained his diploma in physics at the University of Erlangen, Germany, in 1989. He graduated with a Ph.D. on vacuum STM investigations on phase transitions in surface systems in 1992 at the Fritz-Haber-Institute of the Max-Planck-Society in Berlin, Germany. During the following two years he joined the groups of Prof. K. Kern, EPF Lausanne, Switzerland, and Prof. I. K. Robinson, University of Illinois, performing postdoctoral studies on surface alloying and X-ray diffraction on surfaces. Currently, he is a senior scientist at the Fritz-Haber-Institute in the department of Prof. G. Ertl. The current research activities of his group are focused on electrochemical mircromachining, ultrafast electrochemical reaction kinetics, and ordering processes in surface systems, in both electrochemistry and UHV.

* To whom correspondence should be addressed. E-mail: schuster@fhi-berlin.mpg.de.

† Present address: Debye Institute, Utrecht University, P.O. Box 80000, 3508 TA, Utrecht, The Netherlands.

10.1021/ar000133p CCC: $20.00
Published on Web 04/28/2001

local electrode distance, i.e., the length of the current path through the electrolyte. Therefore, upon application of short voltage pulses, the electrodes' DL can only be charged in locations where the distance between the electrodes is small enough. With nanosecond pulses and concentrated electrolytes, sufficient polarization and subsequent electrochemical reactions occur only for distances in the micrometer range. With appropriate tool electrodes, this allows for the three-dimensional micromachining of essentially all electrochemically active materials.[15]

The second approach is based on the fact that the charging of the DL consumes ions from the electrolyte. Therefore, at very small electrode distances, the ion content in the narrow electrolyte gap becomes considerably depleted upon application of a voltage pulse. With about 1 M electrolytes and polarization by 1 V, this becomes relevant for distances of ≤10 nm. If one considers the electrode arrangement in an electrochemical scanning tunneling microscope (STM) with a conventional Ir tip and a typical tip radius of the order of 1 μm, such a small gap evolves over a lateral width of about 100 nm. Upon application of a short voltage pulse to the tip of an electrochemical STM, the electrolyte in this gap is depleted instantaneously for polarizing the DL. In contrast, the refilling of ions from the bulk of the solution is hampered by the relatively slow lateral diffusion along the small gap. For nanosecond pulses, this prevents the ion redistribution in the electrolyte from equilibration and leads to confinement of the electrochemical reactions to regions only a few nanometers away from the apex of the STM tip.[16,17]

Besides conducting local electrochemistry at the well-defined position of the apex of a STM tip, the application of short voltage pulses allows additional pathways for surface modifications. Due to the small effective size of the electrochemical cell consisting of a STM tip and the surface in nanometer distance, the polarization of the DL proceeds very fast. Since electrochemical reaction rates are exponentially dependent on the potential drop in the DL, reactions can be driven on a time scale barely achievable with other methods. In the absence of mass transport limitations, the deposition or dissolution rates of materials can strongly exceed the rates of metal evaporation in a vacuum. This offers new possibilities for the formation of kinetically determined structures during the equilibration of the system. In section IV, we present data on the ordering process of a thermodynamically unstable Au adatom gas. Half a monolayer of Au atoms from the topmost Au(111) surface was removed within a short pulse to the tip of an electrochemical STM. The remaining Au adatom gas decayed into a labyrinthine pattern of Au islands, typical for the spinodal decomposition of a two-phase system. This is completely different from the morphologies expected upon nucleation and growth of a new phase, which usually governs "slow" deposition of materials, both in electrochemistry and in vacuum deposition.

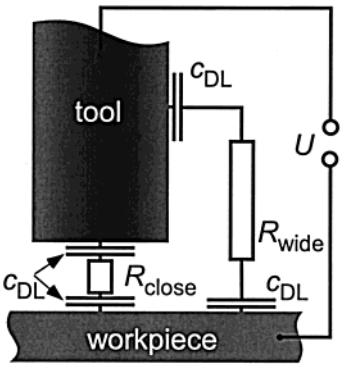

FIGURE 1. Sketch of the electrochemical cell formed by tool and workpiece electrode. Upon application of a voltage pulse, the DL capacity (c_{DL}) is charged with varying time constants, due to the position-dependent electrolyte resistance (R_{close} and R_{wide}) (after ref 15).

II. Electrochemical Micromachining

The three-dimensional machining of metals and semiconductors on micrometer and submicrometer scales is a hitherto only partly solved problem. Lithographic methods are mainly limited to 2D structures. Other methods such as ion beam milling and laser ablation either are relatively slow or provide only limited resolution.[18] We employed an electrochemical technique in which the electrochemical reactions on the electrodes are locally confined with down to submicrometer precision.[15] Upon application of voltage pulses to two electrodes immersed in electrolyte, the DLs on the electrode surfaces charge with a time constant τ proportional to the double-layer capacity C and the electrolyte resistance R (Figure 1). The latter is given by the specific electrolyte resistance ρ and the length of the current path in solution, i.e., the local electrode separation d. Hence, $\tau = RC = \rho d c_{DL}$, where c_{DL} denotes the specific DL capacity. For an electrode arrangement as sketched in Figure 1, the length of the current path and therefore also the charging time constant vary with the position on the workpiece. Consequently, upon application of short voltage pulses, the peak voltage drop in the DL also becomes dependent on the position on the workpiece. Since the electrochemical reaction rate is exponentially dependent on this voltage drop in the DL, the electrochemical reactions are strongly confined to electrode regions exhibiting significant charging, i.e., electrode regions in close proximity.

The above equation directly yields an estimate of the expected machining precision. For example, with typical values of $\rho = 30\ \Omega\cdot$cm (0.1 M $HClO_4$), $c_{DL} \approx 10\ \mu$F/cm^2 for metal electrodes, and pulse durations of $T = 30$ ns, the maximum distance d, where significant charging of the DL is achieved, is calculated to be $d \approx 1\ \mu$m. This can be used, e.g., for the local etching of a workpiece: the application of positive pulses of sufficient pulse height to the workpiece, respectively negative ones to the tool electrode, may induce the electrochemical dissolution of the workpiece within a distance of ≈1 μm from the tool electrode. Feeding the tool electrode similarly to the cutter in a mechanical milling machine allows for the direct

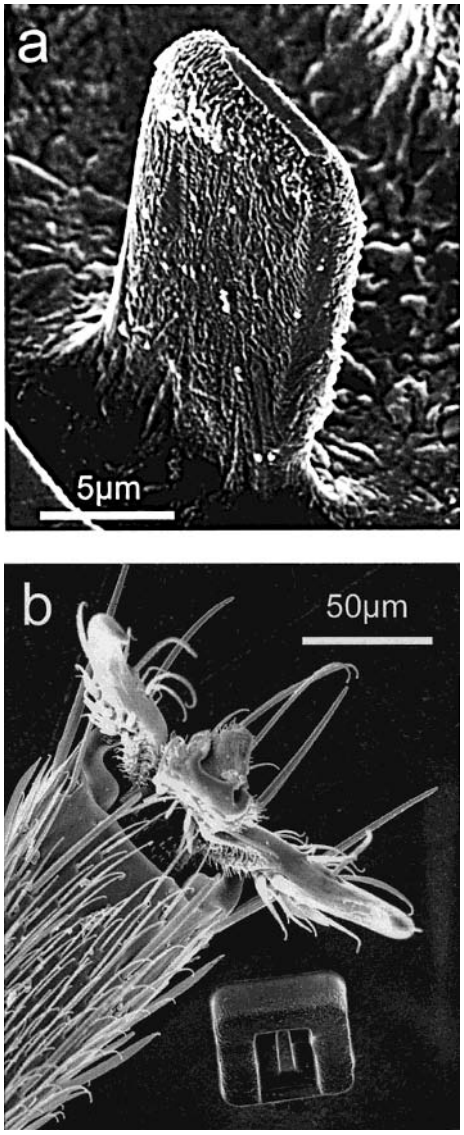

FIGURE 2. (a) Scanning electron micrograph of a Cu tongue with a thickness of 2.5 μm, etched by a 2-MHz sequence of 50-ns, −1.6-V pulses. The tool was a 10-μm-diameter mechanically flattened Pt wire, immersed in 0.01 M $HClO_4$ and 0.1 M $CuSO_4$ (after ref 15). (b) Cu prism etched similar to (a). For comparison, the leg of an ant is arranged next to it.

three-dimensional machining of the workpiece. This is demonstrated in Figure 2, depicting a Cu tongue (Figure 2a) and a small Cu prism next to the leg of an ant (Figure 2b), which were machined out of a Cu substrate, immersed in an aqueous mixture of 0.1 M $CuSO_4$ and 0.01 M $HClO_4$. The tool was a cylindrical 10-μm-diameter Pt wire, the front face of which was mechanically flattened. For mechanical control of the tool-workpiece position, the electrochemical cell was mounted onto a piezo-driven $x-y-z$ stage. Upon application of a 2-MHz sequence of 50-ns, −1.6-V pulses, the tool electrode was first etched vertically into the surface. Afterward, it was fed along a rectangular path to dissolve the groove out of the Cu sheet. The whole procedure took a few minutes, corresponding to about 10^9 pulses. To avoid large-scale corrosion of the Cu sheet, its electrochemical potential was kept at the $Cu|Cu^{2+}$ equilibrium potential by a low-frequency potentiostat that was insensitive to the short voltage pulses. The average potential of the tool was adjusted to +200 mV vs $Cu|Cu^{2+}$ to avoid the deposition of Cu on the tool.

The method can, in principle, be applied to all electrochemically active materials. We successfully structured Co, stainless steel, and p-doped Si surfaces. While Co behaves very similarly to Cu, both stainless steel and Si surfaces evolve stable passivation layers upon oxidation. These have to be removed chemically, which for the case of Si works well with hydrofluoric acid. Also, the inverse process of the etching, the local deposition of Cu, became possible.

The most prominent features of the structures in Figure 2 are the sharp corners and the smooth vertical walls, which result in a high aspect ratio. The grooves are about 14 μm wide. Considering the tool diameter of 10 μm, this results in a distance $d = 2$ μm between tool and workpiece, above which the etching effectively ceases, in good agreement with the above approximation. The actual machining precision of the structures in Figure 2 is indicated by the smooth surface of the Cu tongue, whose roughness is in the 100 nm range, rather than by the tool−workpiece gap. For a quantitative calculation of the machining precision, the real local reaction rate, including mass transport limitations in the small gap, and the geometrical arrangements of the electrodes have to be taken into account. In the case of copper, it turned out that the Cu dissolution rate is limited by mass transport in the small gap; hence, the actual pulse voltage has only a limited influence on the machining precision. In contrast, for stainless steel surfaces, due to the passivating layer, the dissolution rate is very sensitive on the applied pulse voltage, the careful adjustment of which therefore allows for improved spatial resolution.

However, in all cases the above approximation gives a reasonable estimate for the spatial resolution. Furthermore, it correctly represents the correlation between pulse length, electrolyte concentration, and machining precision: The maximum distance of the electrodes, where significant charging occurs, is proportional to the pulse length and the specific electrolyte resistance. Shorter pulses and lower electrolyte concentration therefore achieve better spatial resolution, proven for the etching of holes in a Cu film.[15] In principle, with an infinitely short pulse length or diluted electrolytes, the spatial resolution approaches zero. This is, however, limited, if the DL capacity cannot be charged due to a lack of ions in the small gap between the electrodes. Upon polarization of the DL of a typical metal (c_{DL} = 10 $\mu F/cm^2$) by 1 V, about 0.1 monolayer (ML) of ions is consumed (a coverage of 1 ML corresponds to one ion per substrate surface atom.). Therefore, the concentration of the electrolyte has to be chosen high enough to avoid significant depletion. Taking these considerations into account, employing a 0.3 M electrolyte together with (technically available) 100-ps pulses should achieve a spatial machining resolution in the 10 nm range. An even shorter pulse length, accompanied by an electrolyte of higher concentration, should further improve the spatial resolution. However,

the depletion of the electrolyte in the small gap between two electrodes might be employed itself to confine electrochemical reactions on the electrode surfaces, as shown in the next section.

III. Formation of Single Holes and Cu Clusters on a Au(111) Surface

The above method for electrochemical machining with ultrashort voltage pulses is based on the time and geometry dependence of the DL charging. Its intrinsic limit is the availability of a sufficient amount of ions in the tool−workpiece gap to charge the DL. Even with concentrated electrolytes of 1 M concentration, only every 50th particle is an ion of the respective kind. Therefore, the gap width, which has to be maintained to have a sufficient reservoir of ions for the polarization of the DL, amounts to a few nanometers. Below that width, the depletion of the electrolyte results in an enhanced specific electrolyte resistance, which in the extreme suppresses the Faradaic current, i.e., the electrochemical reactions on the electrode surfaces. The latter ones are then restricted to areas where the two electrodes effectively touch; i.e., the two DLs penetrate each other, and the thickness of the electrolyte approaches zero.

Such a geometrical electrode arrangement is given in an electrochemical STM: The apex of the STM tip, which is a rather macroscopic object, resides at less than 1 nm distance from the substrate surface. Since in our experiments we used mechanically ground Ir wires with a typical tip radius of about 1 μm, the actual geometry in the vicinity of the tip apex resembles an extended gap with a slightly varying gap width, increasing from below 1 nm at the tip apex to about 10 nm at a lateral distance of several hundred nanometers. Upon application of voltage pulses, the electrochemical reactions are expected to be confined to the very apex of the STM tip where the tunneling of electrons also occurs.[16]

For experimental verification, a flame-annealed Au film was used as a substrate, exhibiting large (111) terraces, separated by monatomic steps. The electrolyte was 1 M $CuSO_4$ and 0.5 M H_2SO_4. Figure 3a shows the results of the introduction of four single 50-ns, −2-V pulses to the STM tip. In this STM image, an arrow indicates the in situ formation of a hole with about 5 nm diameter and a depth between 1 and 3 monatomic layers, exactly at the tunneling position of the tip where the pulse was applied. Since the slow scan direction was directed upward, only the upper half of the hole is imaged. The three holes in the upper part of the image were previously produced by three single pulses. During the application of the short voltage pulse, the feedback loop of the STM was switched off, and a high-frequency network was switched onto the STM tip. The application of the pulse interrupted the STM imaging for only a few milliseconds, which is less than 1% of the time for recording a single scan line.

Due to the high electrolyte concentration and the small tip−surface gap, the polarization of the DLs and the consequent depletion of the electrolyte in the small gap

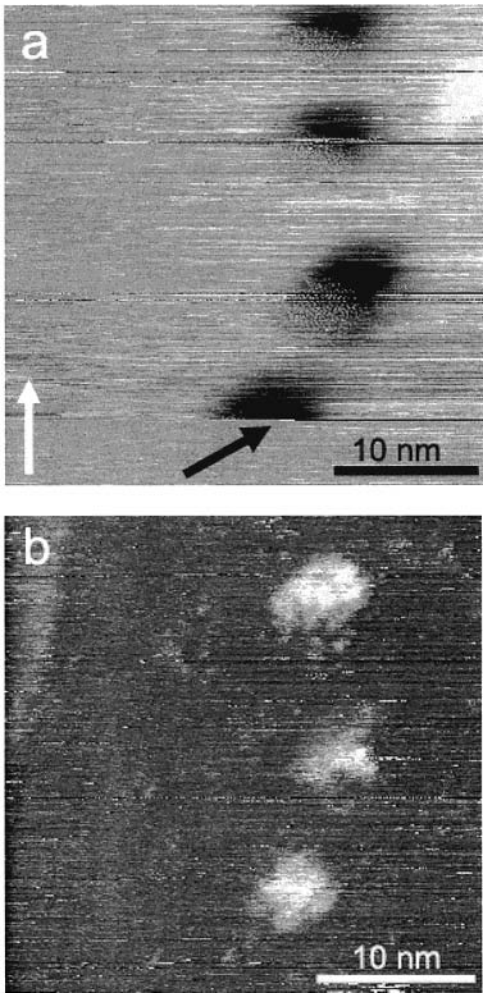

FIGURE 3. (a) In situ formation of a single hole on Au(111) by a 50-ns, −2-V pulse in 1 M $CuSO_4$ and 0.5 M H_2SO_4. The hole is formed at the location of the tip during the application of the pulse (black arrow). The slow scan direction points upward. The three holes in the upper part of the image were previously produced (tunneling voltage, $U_T = -300$ mV; tunneling current, $I_T = 1$ nA). (b) Three single Cu clusters on Au(111) formed by three 50-ns, 3-V pulses to the STM tip in 1 M $CuSO_4$ and 0.5 M H_2SO_4 ($U_T = 230$ mV, $I_T = 1$ nA) (after ref 16).

proceeds very fast, within the first few nanoseconds of the pulse. Significant equilibration of the ion concentration in the small gap is hampered by the long lateral distances and the slow diffusion, compared with those of the migration process. Indeed, typical diffusion constants of about 10^{-5} cm^2/s result in a diffusion length of 10 nm per 100 ns. The depleted solvent layer in the gap can hence be explained as local isolation of the macroscopic tip, which prevents Faradaic currents from flowing and therefore suppresses the electrochemical Au oxidation over most of the gap region. Only at the very apex of the tip, where the electrode distance is merely a few diameters of a solvent molecule, this simplified picture of DLs at the electrodes and an electrolyte between them is no longer applicable. Here, the distance between the ions in the DLs is of the same order of magnitude as the distance between the electrodes, and the notion of an electrolyte resistance is meaningless. It is expected that direct transitions of ions

from one electrode to the counter electrode and vice versa become possible in the local electric field. Only at this location does the electrochemical reaction proceed, and, e.g., the Au surface is locally dissolved.

To check the influence of the electrolyte on the local confinement of the reaction, we conducted experiments in various electrolytes such as H_2SO_4, HCl, KCl, $NaSO_4$, $CuSO_4$, and some of their mixtures. It turned out that the most important prerequisite for the local surface modification was the use of highly concentrated electrolytes. In pure water, hole formation was impossible with ultrashort voltage pulses, which rules out a purely field-induced surface modification due to the high field strength at the tip apex and further supports the electrochemical nature of the process. For an ultimate proof, it had to be checked whether, upon inversion of the pulse polarity, the opposite reaction of the hole formation, i.e., the reduction and deposition of ions from the solution, also becomes possible. This is shown in Figure 3b on a Au(111) surface immersed in 0.5 M $CuSO_4$. Introduction of three short, positive voltage pulses to the tip (50 ns, +4 V) led to the formation of three Cu clusters with about 5 nm diameter and monatomic height. The clusters are located exactly at the positions where the tip was tunneling at the moment when the pulses were applied. These clusters dissolved completely after the sample potential was increased to about 400 mV vs $Cu|Cu^{2+}$, substantiating that they do, indeed, consist of copper and do not constitute contamination disposed off the tip. The potential of the tip was held at about 400 mV vs $Cu|Cu^{2+}$ prior to the application of the pulse, which excludes underpotential deposition of Cu on the tip. Therefore, the deposited Cu had to stem directly from reduction of ions of the electrolyte.

The local electrochemistry resulting from ultrashort voltage pulses differs significantly from other electrochemical approaches for producing small structures with the help of a STM, reviewed, e.g., in refs 19−21. One of these involved the electrochemical plating of the tunneling tip with Cu and the successive mechanical detachment of Cu clusters on the surface by mechanical contact.[22] In a recent experiment, millisecond voltage pulses have been employed to redissolve material from the tip (in this case Co), where it was previously deposited.[23] This led to a local, transient enhancement of the metal ion concentration and therefore to local variations of the Nernst potential for its bulk deposition on the surface. Although this process is, in principle, determined by the diffusion properties of the species, the achieved resolution is about 20 nm with good reproducibility. Other experiments concern the structuring of surfaces in humid air by use of a STM tip. However, in such experiments on Au(111), voltage pulses to the STM tip longer than 100 ms were necessary for nanometer hole formation.[24,25] Therefore, in this case, the local confinement of the reaction has probably to be attributed to the formation of a small water neck between the tip and the surface due to capillary forces, as proposed in recent experiments on the oxidation of Si and Ti.[26,27] Similarly, conductive polymer films have been employed as electrolyte, which allowed both the etching of the substrate and the deposition of metal lines with a thickness down to 200 nm.[28] Also here, the contact area between STM tip and film surface determines the size of the structures.

A different approach for producing single small metal clusters on a surface was successfully demonstrated for the formation of Ag clusters on a graphite surface. The Ag clusters were deposited from a Ag^+-containing solution by applying positive voltage pulses of 50 μs duration to the STM tip.[29,30] The local metal deposition started a few microseconds after the beginning of the pulse and was attributed to nucleation of a Ag cluster in a small hole on the graphite surface formed instantaneously during the application of the pulse. On graphite, the hole formation proceeds independently of the polarity of the pulse, which points to a field effect rather than to electrochemical oxidation of the surface. Analogously, we demonstrated that holes on a Au surface produced by ultrashort voltage pulses can serve as local nucleation sites for Cu bulk deposition.[17]

In conclusion, carrying out electrochemical reactions far from equilibrium conditions, i.e., far from the equilibration of the ion distribution in the electrolyte, can, indeed, lead to strongly localized surface modifications on the nanometer scale. Technological applications comparable to those of e-beam lithography might be possible but still suffer from relatively low processing speed, due to the sequential nature of the modification process.

IV. Structure Formation upon Ordering Processes in Electrochemistry

For many applications, a well-defined size distribution of the fabricated surface features is more important than their definite location. Such a surface morphology can, for example, be achieved by nucleation and growth processes: Semiconducting quantum dots with high monodispersity were recently synthesized by a hybrid electrochemical/chemical method by which small metal islands were first electrochemically deposited onto a graphite surface and afterward chemically transformed into a semiconducting compound.[31] Similar to thin film growth under vacuum conditions, the electrochemical deposition of materials is mostly governed by the nucleation of islands, i.e., by surmounting a nucleation barrier for the formation of a critical nucleus of a condensed phase from a supersaturated adatom gas. This leads to the formation of rather compact, round islands, the size and distance distribution of which are determined by the deposition rate, the diffusivity of the adatoms on the surface, and the size of the critical nucleus for island formation.[32]

However, there exists a different pathway for the condensation of islands from an adatom gas. At high enough adatom densities, the system becomes thermodynamically unstable, and the condensation into the dense phase proceeds instantaneously without surmounting a nucleation barrier.[33,34] The morphology of the system resulting from this so-called spinodal decomposition is

expected to be completely different from those occurring upon nucleation and growth. Cahn and Hillard showed that thermally induced density fluctuations of a certain length scale will exponentially grow with time. Due to the high driving force (i.e., excess free energy), spinodal decomposition typically results in labyrinthine, interwoven patterns, which are never observed during slow, thermally activated nucleation and growth.

The experimental observation of such labyrinthine patterns during thin-layer growth is usually hampered by the slow rate for changing the adatom concentration. Upon changing the adatom surface concentration from its equilibrium value, the system enters the metastable region of the phase diagram. With proceeding supersaturation of the adatom gas, the nucleation barrier and the size of the critical nucleus also shrink, which eventually leads to nucleation and growth of the new phase before the unstable region of the phase diagram can be reached. Hence, thin-layer formation upon evaporation of materials in a vacuum or slow deposition in electrochemistry is governed by the typical patterns of nucleation and growth, with wide variations reaching from dendritic growth to regularly shaped islands.

However, electrochemistry offers the possibility to drive reactions extremely fast. In a small electrochemical cell, like the tip−surface configuration of an electrochemical STM, the DL can be rapidly polarized. Electrochemically induced surface modifications can be observed in situ. For example, in Cl^--containing electrolyte, Au atoms can be dissolved in the electrolyte during a 20 μs, −4 V pulse to the STM tip (Figure 4). The pulse was applied in the center of the STM image in Figure 4a while slowly scanning downward. To allow for large-scale reaction and unconstrained transport of ions in the electrolyte, the tip was retracted by about 2 nm during the application of the pulse. An interconnected, labyrinthine pattern of monatomically high Au islands formed on the surface. Comparison with images taken before revealed that 0.5 ML of Au atoms, only from the topmost terraces, was dissolved during the pulse without changing the terrace structure of the surface. Subsequently, the remaining 0.5 ML of Au atoms in the topmost layer ordered into a labyrinthine pattern.

This pattern rather points to the spinodal decomposition of an unstable, instantaneously created Au adatom gas, in contrast to the conventional nucleation and growth scheme. It is conceivable that upon the application of the high potential step, Au atoms from the topmost surface layer were randomly removed, leaving behind an unstable Au adatom gas with a density of 0.5 ML. Since the dissolution of the material occurred about 6 times faster than the change of the adatom concentration with conventional vacuum or electrochemical methods, the metastable region of the phase diagram was surpassed before nucleation and growth of round and compact Au islands could start. Indeed, assuming that the particle interactions in the Au atom gas are dominated by nearest-neighbor interactions, a density of 0.5 ML equals the critical density;[35] i.e., the adatom gas with 0.5 ML density is situated right in the middle of the coexistence region, where it is definitely unstable.

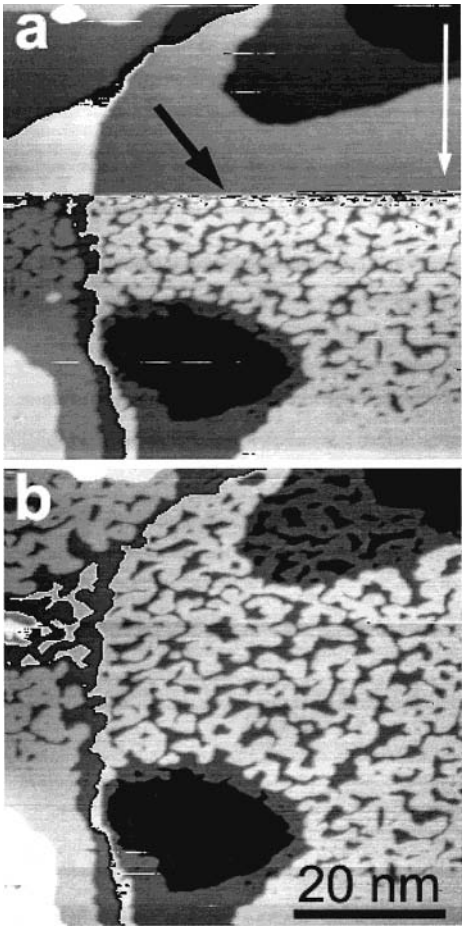

FIGURE 4. (a) During scanning a Au(111) surface in 4 M KCl, the application of a 20-μs, −4-V pulse to the STM tip (black arrow) led to the formation of a labyrinthine pattern of Au islands, reminiscent of structures expected upon spinodal decomposition of an unstable system (the slow scan direction is directed downward). About 0.5 ML of the topmost Au layer was electrochemically dissolved during the short pulse. (b) In the consecutive STM image (1 min later), the pattern coarsened slightly ($U_T = -150$ mV, $I_T = 1$ nA).

The labyrinthine pattern slowly coarsens on a time scale of minutes (Figure 4b). Eventually, after about 30 min, the pattern breaks up into single, compact islands, and Ostwald ripening sets in, where big islands grow at the expense of smaller ones (images not shown here). At this late stage of the ordering process, the surface morphology indeed resembles that resulting from typical nucleation and growth scenarios. The interwoven, labyrinthine patterns were obtained only immediately after the very fast change of the Au adatom concentrations. This became possible due to the small size of the effective electrochemical cell, consisting of the STM tip and the surface in nanometer proximity, which allowed for the unprecedentedly fast polarization of the DL.

V. Conclusions

Applying ultrashort voltage pulses to small electrodes opens two principally different avenues for surface modi-

fications. First, the electrochemical reactions can be confined to surface areas on the micro- to nanometer scale, because of both the spatially confined charging of the DL and the unequilibrated ion distribution in the electrolyte. Second, the small size of the effective cell volume allows for a very fast polarization of the DL and therefore an unprecedented speed of the electrochemical reactions. This might drive the system into regions of the phase diagram which were hitherto impossible to reach, due to kinetic limitations. The ordering process upon the decay of a thermodynamically unstable system may lead to surface morphologies completely different from those observed upon close-to-equilibrium procedures governed by nucleation and growth. Future investigations may include the in situ study of the early time behavior of such ordering processes as well as the study of the electrochemical reaction kinetics itself by directly measuring the current transient flowing through such a small but fast electrochemical cell, e.g., consisting of the tip and surface in an electrochemical STM.

The authors gratefully thank Professor Ertl for his steady support and for many helpful discussions. Dr. A. Bittner's help during the early stages of the STM experiments is gratefully acknowledged. We also heartily thank Drs. P. Allongue and L. Cagnon for their participation in the electrochemical microstructuring experiments.

References

(1) Brus, L. Quantum crystallites and conlinear optics. *Appl. Phys. A* **1991**, *53*, 465−474.
(2) Kastner, M. A. Artificial atoms. *Phys. Today* **1993**, *46*, 24−31.
(3) Colvin, L. V.; Schlamp, M. C.; Allvisatos, A. P. Light-emitting diodes made from cadmium selenide nanocrystals and a semiconducting polymer. *Nature* **1994**, *370*, 354−356.
(4) Boudart, M.; Djéga-Mariadassou, G. *Kinetics of Heterogeneous Catalytic Reactions*; Princeton University Press: Princeton, NJ, 1984.
(5) Takaghara, T. Quantum dot lattice and enhanced excitonic optical nonlinearity. *Surf. Sci.* **1992**, *267*, 310−314.
(6) Kagan, C. R.; Murray, C. B.; Nirmal, M.; Bawendi, M. G. Electronic energy transfer in CdSe quantum dot solids. *Phys. Rev. Lett.* **1996**, *76*, 1517−1520.
(7) Cross, M. C.; Hohenberg, P. C. Pattern formation outside of equilibrium. *Rev. Mod. Phys.* **1993**, *65*, 851−1091.
(8) Erley, G.; Gorer, S.; Penner, R. M. Transient photocurrent spectroscopy: Electrical detection of optical absorption for supported semiconductor nanocrystals in a simple device geometry. *Appl. Phys. Lett.* **1998**, *72*, 2301−2303.
(9) Gorer, S.; Hsiao, G. S.; Anderson, M. G.; Stiger, R. M.; Lee, J.; Penner, R. M. A hybrid electrochemical/chemical synthesis of semiconductor nanocrystals on graphite: a new role for electrodeposition in materials synthesis. *Electrochim. Acta* **1999**, *43*, 2799−2809.
(10) Andriacacos, P. C. Copper on-chip interconnections. *Electrochem. Soc. Interface* **1999**, *8*, 32−37.
(11) Bard, A. J.; Denuault, G.; Lee, C.; Mandler, D.; Wipf, D. O. Scanning electrochemical microscopy: A new technique for the characterization and modification of surfaces. *Acc. Chem. Res.* **1990**, *23*, 357−363.
(12) Mandler, D. M.; Bard, A. J. A new approach to the high-resolution electrodepositions of metals via the feedback mode of the scanning electrochemical microscope. *J. Electrochem. Soc.* **1990**, *137*, 1079−1086.
(13) Bard, A. J.; Fan, F.-R.; Mirkin, M. V. Scanning electrochemical microscopy. *Electroanal. Chem.* **1994**, *18*, 243−377.
(14) Bockris, J. O. M.; Reddy, A. K. N. *Modern Electrochemistry*; Plenum Press: New York, 1970; Vol. II.
(15) Schuster, R.; Kirchner, V.; Allongue, P.; Ertl, G. Electrochemical micromachining. *Science* **2000**, *289*, 98−101.
(16) Schuster, R.; Kirchner, V.; Xia, X. H.; Bittner, A. M.; Ertl, G. Nanoscale electrochemistry. *Phys. Rev. Lett.* **1998**, *80*, 5599−5602.
(17) Xia, X. H.; Schuster, R.; Kirchner, V.; Ertl, G. The growth of size-determined Cu clusters in nanometer holes on Au(111) due to a balance between surface and electrochemical energy. *J. Electroanal. Chem.* **1999**, *461*, 102−109.
(18) *Handbook of Microlithography, Micromachining, & Microfabrication*; Rai-Coudhury, P., Ed.; SPIE Optical Engineering Press: Bellingham, WA, 1997.
(19) Staufer, U. In *Scanning Tunneling Microscopy II*; Güntherodt, H.-J., Wiesendanger, R., Eds.; Springer: Berlin, 1992.
(20) Wiesendanger, R. Contributions of scanning probe microscopy and spectroscopy to the investigation and fabrication of nanometer-scale structures. *J. Vac. Sci. Technol.* **1994**, *B12*, 515−529.
(21) Nyffenegger, R. M.; Penner, R. M. Nanometer-scale surface modification using the scanning probe microscope: progress since 1991. *Chem. Rev.* **1997**, *97*, 1195−1230.
(22) Kolb, D. M.; Ullmann, R.; Will, T. Nanofabrication of small copper clusters on gold(111) electrodes by a scanning tunneling microscope. *Science* **1997**, *275*, 1097−1099.
(23) Hoffmann, D.; Schindler, W.; Kirschner, J. Electrodeposition of nanoscale magnetic structures. *Appl. Phys. Lett.* **1998**, *73*, 3279−3281.
(24) Lebreton, C.; Wang, Z. Z. Nanowriting on an atomically flat gold surface with scanning tunneling microscope. *Scan. Microsc.* **1994**, *8*, 441−448.
(25) Lebreton, C.; Wang, Z. Z. Critical humidity for removal of atoms from the gold surface with scanning tunneling microscopy. *J. Vac. Sci. Technol.* **1996**, *B14*, 1356−1359.
(26) Avouris, P.; Hertel, T.; Martel, R. AFM tip-induced local oxidation of silicon: kinetics, mechanism, and nanofabrication. *Appl. Phys. Lett.* **1997**, *71*, 285−287.
(27) Sugimura, H.; Uchida, T.; Kitamura, N.; Masuhara, H. Scanning tunneling microscope tip-induced anodization for nanofabrication of titanium. *J. Phys. Chem.* **1994**, *98*, 4352−4357.
(28) Hüsser, O. E.; Craston, D. H.; Bard, A. J. High-resolution deposition and etching of metals with a scanning electrochemical microscope. *J. Vac. Sci. Technol. B* **1988**, *6*, 1873−1876.
(29) Li, W.; Virtanen, J. A.; Penner, R. M. Nanometer-scale electrochemical deposition of silver on graphite using a scanning tunneling microscope. *Appl. Phys. Lett.* **1992**, *60*, 1181−1183.
(30) Li, W.; Hsiao, G. S.; Harris, D.; Nyffenegger, R. M.; Virtanen, J. A.; Penner, R. M. Mechanistic study of silver nanoparticle deposition directed with the tip of a scanning tunneling microscope in an electrolytic environment. *J. Phys. Chem.* **1996**, *100*, 20103−20113.
(31) Penner, R. M. Hybrid electrochemical/chemical synthesis of quantum dots. *Acc. Chem. Res.* **2000**, *33*, 78−86.
(32) Brune, H. Microscopic view of epitaxial metal growth: nucleation and aggregation. *Surf. Sci. Rep.* **1998**, *31*, 121−230.
(33) Gunton, J. D.; Miguel, M. S.; Sahni, P. S. The dynamics of first-order phase transitions. In *Phase Transitions and Critical Phenomena*; Domb, C., Lebowitz, J. L., Eds.; Academic Press: London, 1983; Vol. 8, pp 267−466.
(34) Binder, K. Theory of first-order phase transitions. *Rep. Prog. Phys.* **1987**, *50*, 783−859.
(35) Bell, G. M.; Lavis, D. A. *Statistical Mechanics of Lattice Models*; Ellis Horwood Limited: Chichester, 1989.

AR000133P